

Reexamining the "finite-size" effects in isobaric yield ratios using a statistical abrasion-ablation model

C. W. Ma^{1,*}, S. S. Wang¹, H. L. Wei¹, and Y. G. Ma^{2†}

¹*Department of Physics, Henan Normal University, Xinxiang 453007*

²*Department of Nuclear Physics, Shanghai Institute of Applied Physics,
Chinese Academy of Sciences, Shanghai 201800*

(Dated: October 9, 2018)

The "finite-size" effects in the isobaric yield ratio (IYR), which are shown in the standard grand-canonical and canonical statistical ensembles (SGC/CSE) method, is claimed to prevent obtaining the actual values of physical parameters. The conclusion of SGC/CSE maybe questionable for neutron-rich nucleus induced reaction. To investigate whether the IYR has "finite-size" effects, the IYR for the mirror nuclei [IYR(m)] are reexamined using a modified statistical abrasion-ablation (SAA) model. It is found when the projectile is not so neutron-rich, the IYR(m) depends on the isospin of projectile, but the size dependence can not be excluded. In reactions induced by the very neutron-rich projectiles, contrary results to those of the SGC/CSE models are obtained, i.e., the dependence of the IYR(m) on the size and the isospin of the projectile is weakened and disappears both in the SAA and the experimental results.

PACS numbers: 25.70.Pq, 21.65.Cd, 25.70.Mn, 24.60.-k

Keywords: finite effect, neutron-rich nucleus, isobaric method

The yield of fragments has been demonstrated as a powerful tool to study the information of nuclear matter and temperature in heavy-ion collisions (HIC). For instance, the scaling of the ratios between the isotopic yields in reactions of similar measurements, namely the isoscaling, has been extensively used to study the symmetry energy of hot emitting source in the framework of various theoretical models as well as in experiments [1–11]. In addition, the kinetic energy spectra of light particles and the double yield ratio of light fragments are taken as thermometers [12–19].

Using a modified Fisher model (MFM), which bases on the free energy [20], the isobaric yield ratio (IYR) is used to study the symmetry energy of the fragments [21–25]. The correlation between the IYR and energy term which contributes to the free energy of the fragment is constructed to extract the physical parameters associated with the mass of nucleus [26]. In the IYR method, the energy terms which only depend on mass cancel out, thus makes it convenient to investigate the symmetry-energy term in the mass formula. However, it is claimed that the IYR method, which utilizes only one reaction system, does not provide cancelation or minimization of the effects associated with mass and charge constraints due to the "finite-size" effects in the standard grand-canonical and canonical statistical ensembles (SGC/CSE) methods [27].

The linear behavior of the IYR for the mirror nuclei [IYR(m)], which is discussed in Refs. [21, 26, 27], is as follows,

$$\begin{aligned} IYR(m) &= \ln[R(I + 2, I, A)] = \ln[R(1, -1, A)] \\ &\equiv \ln[Y(A, 1)/Y(A, -1)] = [(\mu_n - \mu_p) + a_c \cdot x]/T, \end{aligned} \quad (1)$$

where $I = N - Z$ is the neutron-excess, a_c is the Coulomb-energy coefficient, $x \equiv 2(Z - 1)/A^{1/3}$, μ_n and μ_p are the neutron and proton chemical potentials, respectively. This equation suits for both the SGC/CSE and MFM theories.

Depending on the volume of the reaction system, it was claimed that the "finite-size" effects of the IYR(m) in SGC/CSE prevent one from obtaining precise information on the nuclear properties using the isobaric ratio method, and the "finite-size" effects are negligible only for system sizes much larger than those actually formed [27]. Actually, in the similar isoscaling method, though the finite size effect is believed to be minimized from the sources with the fixed N/Z , it is still obvious in the isoscaling in some models [9].

The yields of the fragments strongly depends on the isospin, as well as the neutron and proton density (ρ_n and ρ_p) distributions of the projectile nucleus. Actually, the ρ_n and ρ_p distributions are important inputs in the nuclear reaction models. However, there is no such information in SGC/CSE [27, 28]. And temperature in SGC/CSE is set to a certain value, but in fact the temperature has a wide distribution observed in light fragments and heavy fragments [10, 13–15]. Different temperature values have been used in similar theories [27, 29, 30]. The yields of fragments in SGC/CSE are not shown in Ref. [27]. Considering the density distributions of neutron-rich nucleus, the SGC/CSE is not a good model to evaluate the yields of fragments in the reactions induced by the neutron-rich nucleus using the generalized parameters. Thus the inference based on the yields of fragments in SGC/CSE seems doubtful.

To clarify the possibility of the isospin dependence of IYR(m), in Fig. 1 some IYR(m) for the measured reactions are plotted. The used reactions are the $140A$ MeV $^{40,48}\text{Ca} + ^9\text{Be}$ [31], $1A$ GeV $^{124,136}\text{Xe} + \text{Pb}$ [32], $1A$ GeV

* Email: machunwang@126.com; mobile:15836181225

† Email: ygma@sinap.ac.cn

$^{56}\text{Fe} + p$ [33], $40A$ MeV $^{64}\text{Zn} + ^{112}\text{Sn}$ and $^{70}\text{Zn} + ^{124}\text{Sn}$ [34]. In (a) of Fig. 1, $\text{IYR}(m)$ are for reactions using the neutron-proton symmetric projectiles, which show similar distributions except the ^{40}Ca reaction. When $x > 11$, these $\text{IYR}(m)$ reach plateaus. The $\text{IYR}(m)$ for the ^{64}Zn reaction is different to others maybe due to the projectile-like fragments are removed in the measurements. The $\text{IYR}(m)$ for the ^{124}Xe reaction is plotted in (a) since ^{124}Xe is N/Z symmetric comparing to ^{136}Xe , and actually the $\text{IYR}(m)$ for the ^{124}Xe reaction does show the character of $\text{IYR}(m)$ for those of the N/Z symmetric nuclei reactions. The overlapping $\text{IYR}(m)$ in (b) of Fig. 1 are for the reactions using the neutron-rich projectiles. $\text{IYR}(m)$ for these reactions in Fig. 1 indicate that the finite size effect and the volume effect are negligible in the neutron-rich nucleus induced reaction.

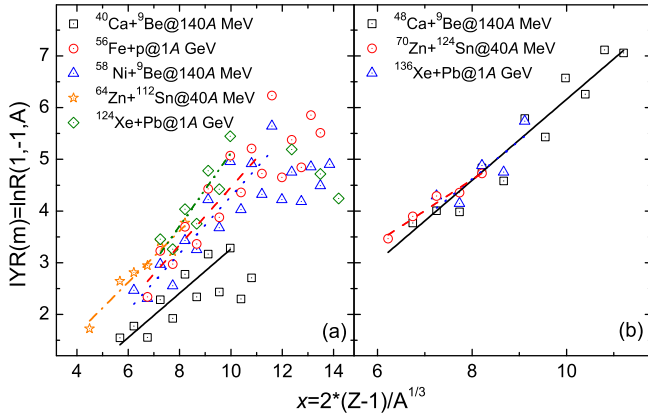


FIG. 1. (Color online) The isobaric yield ratio for mirror nuclei [$\text{IYR}(m)$] in measured reactions. The projectile nuclei are n/p symmetric and neutron-rich in (a) and (b), respectively. The lines denote the linear fitting results of $\text{IYR}(m)$.

The statistical abrasion-ablation (SAA) model well reproduces the yields of fragments in HIC induced by the neutron-rich nucleus [5, 35–40], and it is applied to study the isospin effects in reactions induced by the neutron-rich projectile [38, 39, 41–44]. It can well reproduce the yields of both the small and large mass fragments in the $140A$ MeV $^{40,48}\text{Ca} + ^9\text{Be}$ and $^{58,64}\text{Ni} + ^9\text{Be}$ projectile fragmentation, and the density effect in the fragment yield is investigated [38, 41]. Considering the dependence of the yields and the resultant $\text{IYR}(m)$ on the isospin of the projectile, the "finite-size" effects of the $\text{IYR}(m)$ shown in SGC/CSE (which depends on the volume of the reaction system) should be reexamined. In this article, using the SAA model, the $140A$ MeV $^{38\sim 52}\text{Ca}$ nuclei which have different isospins, and $^{72}\text{Zn}/^{96}\text{Zr}/^{120}\text{Sn}$ which have the same N/Z ratio as ^{48}Ca (which are calculated in Ref. [27]) are re-calculated to demonstrate the dependence of the $\text{IYR}(m)$ on the isospin and mass of the projectile (A_p). For simplification, only important formula of the SAA are listed here since the model is well described in Refs. [35, 36, 38, 39].

The SAA model is a two-stages model, in which the

first stage describes the collisions and determine the primary fragments, and the second stage models the deexcitation of the primary fragments. In the colliding stage, the SAA model takes independent nucleon-nucleon collisions for participants in an overlap zone of the two colliding nuclei and determines the distributions of abraded neutrons and protons. The colliding nuclei are described to be composed of parallel tubes orienting along the beam direction. For an infinitesimal tube in the projectile, the transmission probabilities for neutrons (protons) at a given impact parameter \vec{b} are calculated by

$$t_k(\vec{s} - \vec{b}) = \exp\{-[\rho_n^T(\vec{s} - \vec{b})\sigma_{nk} + \rho_n^P(\vec{s} - \vec{b})\sigma_{pk}]\}, \quad (2)$$

where ρ^T is the nuclear-density distribution of the target integrated along the beam direction, the vectors \vec{s} and \vec{b} are defined in the plane perpendicular to beam, and $\sigma_{k'k}$ is the free nucleon-nucleon reaction cross section. The average absorbed mass in the limit of infinitesimal tubes at a given \vec{b} is,

$$\begin{aligned} \langle \Delta A(b) \rangle = & \int d^2s \rho_n^T(\vec{s}) [1 - t_n(\vec{s} - \vec{b})] \\ & + \int d^2s \rho_p^P(\vec{s}) [1 - t_p(\vec{s} - \vec{b})]. \end{aligned} \quad (3)$$

The ρ_n and ρ_p distributions are assumed to be the Fermi-type. The cross section of a specific isotope (primary fragment) can be calculated from

$$\sigma(\Delta N, \Delta Z) = \int d^2b P(\Delta N, b) P(\Delta Z, b), \quad (4)$$

where $P(\Delta N, b)$ and $P(\Delta Z, b)$ are the probability distributions for the abraded neutrons and protons at a given impact parameter b , respectively.

The second stage of the reaction in the SAA is the evaporation of the primary fragment [36], which is described by the conventional statistical model under the assumption of thermal equilibrium. After the evaporation, the isotopic yield (final fragment) comparable to the experimental result is obtained.

The $\text{IYR}(m)$ of the calculated $140A$ MeV $^{38\sim 52}\text{Ca} + ^{12}\text{C}$ reactions are plotted in Fig. 2. The $\text{IYR}(m)$ in the $^{38\sim 52}\text{Ca}$ reactions increases when the projectile becomes more neutron-rich. Different to the results in SGC/CSE, in which the linear correlation exhibits in the $x > 6$ fragments, the linear correlation exhibits in the fragments of relative small x . Fairly well linear correlations between the $\text{IYR}(m)$ and x are found in the $^{42,44}\text{Ca}$ reactions. For the neutron-deficient ^{38}Ca projectile, the $\text{IYR}(m)$ firstly increases linearly with x when $x < 7$, but decreases when $x > 7$. The $\text{IYR}(m)$ for ^{40}Ca has a similar distribution as that of ^{38}Ca except the inflection x is around 8.5. For the neutron-rich $^{46\sim 52}\text{Ca}$ projectiles, the $\text{IYR}(m)$ increases linearly when x is not large, but it increases quickly when x of fragments is larger than $0.85x$ of projectile. For these fragments, only few nucleons are removed from the projectile, which are mostly produced in the peripheral collisions in the SAA model [42?]. The yield of mirror

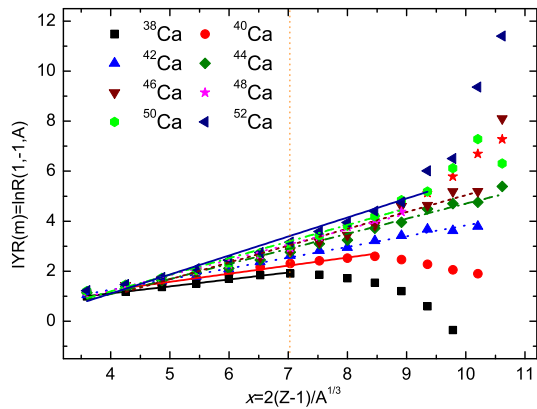


FIG. 2. (Color online) IYR(m) for the 140A MeV $^{38\sim 52}\text{Ca} + ^{12}\text{C}$ reactions calculated by the SAA model. The lines denote the linear fitting results.

nucleus which has small- x and large mass x are affected by ρ_n and ρ_p . The similar IYR(m) shown in the small- x mirror nuclei can be explained as the similarity of the ρ_n and ρ_p distributions in the core of projectiles. The deviation of the IYR(m) shown in the large- x mirror nuclei shows the difference of ρ_n and ρ_p in the surface of projectile, which can also be viewed as a skin effect of the projectile [38, 44]. The slope [only considering the linearly increasing part of the IYR(m)] slightly increases as the neutron numbers of the projectile increases. But for the ^{50}Ca and ^{52}Ca reactions, the IYR(m) almost overlap except for some fragments with large x , which shows a signature of saturation in reactions of very neutron-rich projectile.

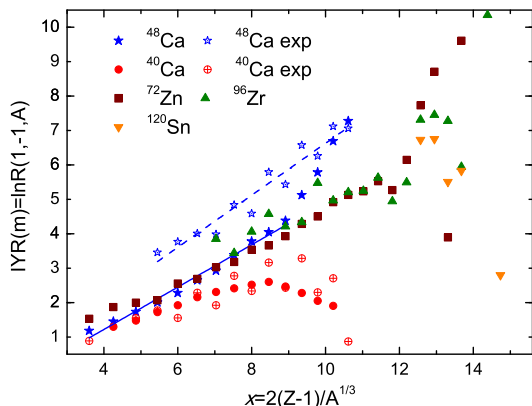


FIG. 3. (Color online) The IYR(m) in reactions calculated using SAA and measured reactions. The full and open circles (stars) are for the SAA and experimental [31] 140A MeV $^{40}\text{Ca}/^{48}\text{Ca}$ reactions, respectively; the triangles, hexagon, and diamonds represent the IYR(m) for the 140A MeV $^{72}\text{Zn}/^{96}\text{Zr}/^{120}\text{Sn} + ^{12}\text{C}$ reactions. The lines are the fitting results by Eq. (1).

In Fig. 3, the SAA and the experimental IYR(m) for the $^{40,48}\text{Ca}$ and the 140A MeV $^{72}\text{Zn}/^{96}\text{Zr}/^{120}\text{Sn} + ^{12}\text{C}$ reactions are plotted. Though the odd-even staggering

in the experimental IYR(m) can not be reproduced, the SAA results can fit the ^{40}Ca experimental data rather well, including the decreasing behavior of IYR(m) when $x > 9$. For ^{48}Ca , the calculated IYR(m) are smaller than those of the experiments. The linear fittings of the SAA and the experimental data read $y = (0.62 \pm 0.02)x - (1.24 \pm 0.16)$ and $y = (0.75 \pm 0.06)x - (0.92 \pm 0.50)$, respectively. More interesting point the figure tells us is that the large difference among the IYR(m) in SGC/CSE in the $^{72}\text{Zn}/^{96}\text{Zr}/^{120}\text{Sn}$ reactions disappears in the SAA results. The IYR(m) for ^{72}Zn projectile exhibits quite good linear correlation when $x < 11$, which shows very little difference from the calculated IYR(m) for ^{48}Ca . The mirror nuclei of small- A do not survive the deexcitation process in the SAA calculation for ^{96}Zr and ^{120}Sn , but the IYR(m)s for ^{72}Zn , ^{96}Zr , and ^{120}Sn show very little difference when $x < 12$. Considering the saturation of the IYR(m) for the reactions induced by neutron-rich nucleus shown in Fig. 1 and 2, the overlapping the IYR(m) for ^{72}Zn , ^{96}Zr , and ^{120}Sn reactions is reasonable.

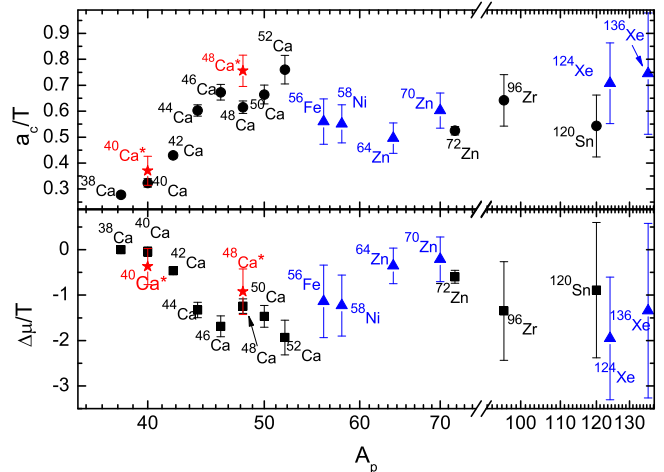


FIG. 4. (Color online) a_c/T and $\Delta\mu/T$ fitted from the IYR(m) by Eq. (1). The x axis represents the mass (A_p) of the projectiles. The labels $^{40}\text{Ca}^*$, $^{48}\text{Ca}^*$, and stars represent the values for the measured results. The triangles represent the values for reactions shown in Fig. 1 except the Ca induced reactions.

In Fig. 4, a_c/T and $\Delta\mu$ from the IYR(m) are plotted. The fittings are limited to the linear part of the IYR(m). a_c/T and $\Delta\mu$ of the $^{64,70}\text{Zn}$ reactions [21] are slightly different to other reactions, which may due to the measurement is limited to the special spatial angles, and the projectile-like fragments are excluded. In the measured reactions, a_c/T ($\Delta\mu/T$) for the ^{56}Fe and ^{58}Ni reactions have very little difference, and the same occurs in the ^{48}Ca and ^{136}Xe reactions. a_c/T ($\Delta\mu/T$) from the IYR(m) for the N/Z symmetric projectile are smaller (larger) than those of the neutron-rich projectile. In the SAA, the a_c/T ($\Delta\mu/T$) of the IYR(m) for the Ca-isotopes increases (decreases) when A_p increases, which shows a kind of isospin dependence. But in reactions of the large-

mass projectiles, the a_c/T ($\Delta\mu/T$) obtained are very similar. a_c/T and $\Delta\mu/T$ tend to be flat and saturate when the projectiles are neutron-rich (after ^{44}Ca). For the projectiles having the same N/Z , no "finite-size" effects for the larger systems ($^{72}\text{Zn}/^{96}\text{Zr}/^{120}\text{Sn}$) are shown in a_c/T or $\Delta\mu/T$. It is easy to conclude that when the projectile is not very neutron-rich, the IYR(m) depends on the isospin of the projectile, but its size dependence cannot be excluded. When the projectile is neutron-rich, the isospin dependence of the IYR(m) is weakened and even disappears, and the size dependence of the IYR(m) can be excluded.

According to Eq. (4), the yield of a primary fragment is mainly determined by the nucleon-nucleon cross sections, the ρ_n and ρ_p distributions. Different to the strictly linear increase of the IYR(m) in the $x > 6$ fragments in SGC/CSE, in the SAA results the IYR(m) in fragments with small x has very little difference, but show sudden changes in the large- x fragments. This is also shown in the measured data in Fig. 1(a). Beside the dependence of the projectile mass, the phenomenon can also be explained as the isospin effects, which is similar to the isospin phenomena shown in HIC [5, 15, 38, 41, 42, 45, 46]. The similarity in the IYR(m) of the small- x fragments can be explained being the similarity of the ρ_n and ρ_p distributions in the central collisions, while the large difference in the IYR(m) of the large- x fragments corresponds to the large difference between the ρ_n and ρ_p distributions in the peripheral collisions according to the skin region of the neutron-rich projectile [38, 44]. It is concluded that both the isospin effects and the size effects are obvious for the not very neutron-rich reactions. But for the very neutron-rich projectile, contrary conclusions to the "finite-size" effects in SGC/CSE are found, i.e., the dependence of the IYR(m) on the system size disappears.

Using one reaction, the extracted $(\mu_n - \mu_p)/T$ and a_c/T

by the IYR method could depend on the N/Z ratio of projectile. In Ref. [21], the a_c/T is scaled to the reaction system parameter Z/A ($\equiv (Z_p + Z_t)/(A_p + A_t)$). If using Huang's methods [21] to extract the a_{sym}/T of the fragments, an increase of 0.15 of a_c/T may introduce a difference of 0.6~1.5 when x increases from 4 to 10, i.e., for the small- x fragment, the difference is rather small. Based on these results, it is suggested that the isobaric yield ratio only has little "finite-size" effects, especially in reactions of very neutron-rich projectile.

To summarize, the "finite-size" effects in the IYR(m) in the SGC/CSE models are reexamined using a modified SAA model by considering the influence of density in the yield of the fragment in HICs. The SAA and the experimental results reveal that, when the projectile is not so neutron-rich, the IYR(m) depends on the isospin of projectile nucleus, but the size dependence of the IYR(m) can not be excluded. When the projectile is very neutron-rich, the IYR(m) dependence of the isospin of projectile is weakened and disappears, and the IYR(m) does not depend on the mass (or volume) of the projectile. The "finite-size" effects shown in SGC/CSE, which depend on the mass or the volume of the projectile, disappear in the reactions induced by the neutron-rich projectile both in the SAA and experimental results.

This work is supported by the National Natural Science Foundation of China under contract Nos. 10905017 and 10979074, the Knowledge Innovation Project of the Chinese Academy of Sciences under contract No. KJCX2-EW-N01, Program for Science&Technology Innovation Talents in Universities of Henan Province (HASTIT), and the Young Teacher Project in Henan Normal University, China. We thank Dr. Mei-Rong Huang and Professor Roy Wada at the Institute of Modern Physics, Chinese Academy of Science of China for providing us the experimental results of the $^{64,72}\text{Zn} + ^{124}\text{Sn}$ reactions.

-
- [1] Tsang M B *et al* 2000 *Phys. Rev. Lett.* **85** 716
[2] Tsang M B *et al* 2006 *Eur. Phys. J. A* **30** 129
[3] Botvina A S *et al* 2002 *Phys. Rev. C* **65** 044610
[4] Zhou P *et al* 2011 *Phys. Rev. C* **84** 037605
[5] Fang D Q *et al* 2007 *J. Phys. G: Nucl. Part. Phys.* **34** 2173
[6] Chen Z *et al* 2010 *Phys. Rev. C* **81** 064613
[7] Ma Y G *et al* 2005 *Phys. Rev. C* **72** 064603
[8] Dorso C O *et al* 2006 *Phys. Rev. C* **73** 044601
[9] Dorso C O 2006 *Phys. Rev. C* **73** 034605
[10] Tian W D *et al* 2005 *Chin. Phys. Lett.* **22** 306
[11] Ono A *et al* 2003 *Phys. Rev. C* **68** 051601(R)
[12] Albergo S *et al* 1985 *Nuovo Cimento A* **89** 1
[13] Ma C W *et al* 2013 *Comm. Theo. Phys.* **59** 95
[14] Su J *et al* 2012 *Phys. Rev. C* **85** 017604
[15] Ma C W *et al* 2012 *Phys. Rev. C* **86** 054611
[16] Natowitz J B *et al* 1995 *Phys. Rev. C* **52** R2322
[17] Wang J *et al* 2005 *Phys. Rev. C* **72** 024603
[18] Ma Y G *et al* 2005 *Phys. Rev. C* **71** 054606
[19] Wada R *et al* 1997 *Phys. Rev. C* **55** 227
[20] Hirsch A S *et al* 1984 *Phys. Rev. C* **29** 508.
[21] Huang M *et al* 2010 *Phys. Rev. C* **81** 044620
[22] Ma C W *et al* 2012 *Eur. Phys. J. A* **48** 78
[23] Ma C W *et al* 2012 *Chin. Phys. Lett.* **29** 062101
[24] Ma C W *et al* 2012 *Chin. Phys. Lett.* **29** 092101
[25] Ma C W *et al* 2013 *Phys. Rev. C* **xx** xxxxxx
[26] Ma C W *et al* 2011 *Phys. Rev. C* **83** 064620
[27] Souza S R, and Tsang M B 2012 *Phys. Rev. C* **85** 024603
[28] Das C B *et al* 2005 *Phys. Rep.* **406** 1
[29] Chaudhuri G *et al* 2007 *Phys. Rev. C* **76** 067601
[30] Tsang M B *et al* 2007 *Phys. Rev. C* **76** 041302(R)
[31] Mocko M *et al* 2006 *Phys. Rev. C* **74** 054612
[32] Henzlova D *et al* 2008 *Phys. Rev. C* **78** 044616
[33] Villagrasa-Canton C *et al* 2007 *Phys. Rev. C* **75** 044603
[34] Huang M R, and Wada R, private communication
[35] Brohm T, and Schmidt K -H 1994 *Nucl. Phys. A* **569** 821
[36] Gaimard J J, and Schmidt K H 1991 *Nucl. Phys. A* **531**

709

- [37] Wei H L and Ma C W 2010 *Acta Phys. Sin.* **59** 5364 (in Chinese)
- [38] Ma C W *et al* 2009 *Phys. Rev. C* **79** 034606
- [39] Fang D Q *et al* 2000 *Phys. Rev. C* **61** 044610
- [40] Ma C W *et al* 2008 *Chin. Phys. B* **17** 1216
- [41] Ma C W *et al* 2009 *Chin. Phys. B* **18** 4781
- [42] Ma C W *et al* 2010 *J. Phys. G: Nucl. Part. Phys.* **37** 015104
- [43] Fang D Q *et al* 2010 *Phys. Rev. C* **81** 047603
- [44] Ma C W *et al* 2010 *Phys. Rev. C* **82** 057602
- [45] Ma C W, and Wang S S 2011 *Chin. Phys. C* **35** 1017
- [46] MA Y G *et al* 1999 *Chin. Phys. Lett.* **16** 256